



Prediction of bearing capacity of H shaped skirted footings on sand using soft computing techniques

T. Gnananandarao ^{a,*}, V.N. Khatri ^b, R.K. Dutta ^a

^a Department of Civil Engineering, National Institute of Technology, Hamirpur, India

^b Department of Civil Engineering, Indian Institute of Technology, Dhanbad, India

* Corresponding e-mail address: anandrcwing@gmail.com

ORCID identifier:  <https://orcid.org/0000-0002-3332-8083> (T.G.)

ABSTRACT

Purpose: The present study aims to apply soft computing techniques, Artificial Neural Network (ANN) and M5P model tree, to predict the ultimate bearing capacity of the H plan shaped skirted footing on the sand

Design/methodology/approach: A total of 162 laboratory test data for the regular plan shaped (square, circular, rectangular, and strip (up to $L/B = 2.5$) skirted footing were collected from the literature to develop the soft computing-based models. These models were later modified for the H Plan shaped skirted footing with the introduction of the multiplication factor. The input variables chosen for the regular plan shaped footings were skirt depth to width of the footing ratio (D_s/B), friction angle of the sand (ϕ), the ratio of the interface friction angle-to-friction angle of sand (δ/ϕ), and length-to-width (L/B) ratio of the footing. The output is the bearing capacity ratio (BCR, a ratio of the bearing capacity of the skirted footing to the bearing capacity of un-skirted footing).

Findings: Sensitivity analysis was carried out to see the impact of the individual variable on the BCR). The sensitivity results reveal that the skirt depth to width of the footing ratio is the primary variable affecting the BCR. Finally, the performance of the developed soft computing models was assessed using six statistical parameters. The results from the statistical parameters reveal that model developed using ANN was performing superior to the one prepared using M5P model tree technique for the prediction of the ultimate bearing capacity of H plan shaped skirted footing on sand.

Research limitations/implications: The model equations are developed with experimental laboratory data. Hence, these equations need further improvement by using field data. However, until now there no field data have been available to include in the present data set.

Practical implications: These proposed model equations can be used to predict the bearing capacity of the H-shaped footing with the help of D_s/B , ϕ , δ/ϕ and L/B without performing the laboratory experiments.

Originality/value: There is no such model equation that was developed so far for the H-shaped skirted footings. Hence, an attempt was made in this article to predict the bearing capacity of the H-shaped footing by using available experimental data with the help of soft computing techniques.

Keywords: Bearing capacity ratio, Sand, Regular plan shaped skirted footings, H plan shaped skirted footings, Artificial neural networks, M5P model tree

Reference to this paper should be given in the following way:

T. Gnananandarao, V.N. Khatri, R.K. Dutta, Prediction of bearing capacity of H shaped skirted footings on sand using soft computing techniques, Archives of Materials Science and Engineering 103/2 (2020) 62-74. DOI: <https://doi.org/10.5604/01.3001.0014.3356>

METHODOLOGY OF RESEARCH, ANALYSIS AND MODELLING

1. Introduction

Structural skirts attached to the regular plan shaped footing are an alternative method for improving the bearing capacity and reducing the settlement. Regular plan shaped skirted footings (square, circular, rectangular, and strip) were extensively used for the offshore structures as their installation is easy in comparison to the deep footing [1-8]. But due to economic and architectural reasons under certain circumstances, the footing with different geometries such as E, T, and H shape in the plan are required. Such footings were termed as multi-edge footings [9]. Laboratory tests on the multi-edge footings without skirt were performed by [9] and reported that the bearing capacity of the multi-edge footings was slightly greater than the bearing capacity of the square footing of the same width. A study on the multi-edge H shaped footing with and without a skirt on the sand was reported by [10] by varying the relative density and the normalized skirt depth from 30 % to 60 % and 0.25 to 1.5 respectively and confirmed the findings of [9] concerning multi-edge footing without a skirt. In order to determine the bearing capacity of such types of footings, the researchers are resorting to experimental investigations as no bearing

capacity equation in literature is available for such types of footings. But generating the data by conducting the experiments is very expensive. An alternative approach can be to build a mathematical model to understand the relationships among the various variables by calibrating and fitting the experimental data generated. The power of soft computing techniques for storing, learning and capturing the complex connection amongst the various variables without any preceding expectations about the bearing capacity ratio makes the soft computing techniques a superior alternative for modeling. Hence, the paper presents the application of soft computing techniques (ANN and M5P model tree) to model the behavior in terms of the bearing capacity ratio of such unconventional H plan shaped multi-edge skirted footing. The schematic of the soft computing techniques and the simple M5P model tree is shown in Fig. 1 (a) and (b) respectively. Hence, in the present paper, the correlation for the H shaped skirted footing was proposed in terms of the bearing capacity of regular shaped skirted footings with the use of soft computing techniques (ANN and M5P model tree). It will help the researchers to calculate the bearing capacity of such unconventional H plan shaped multi-edge skirted footing.

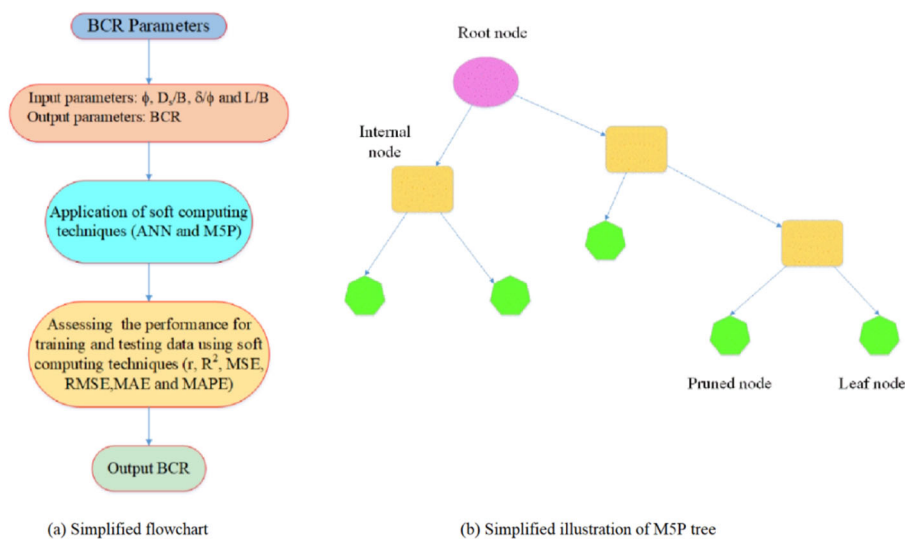


Fig. 1. Simplified illustration of the soft computing techniques and the simple M5P model tree

2. Background

Soft computing techniques such as ANN was initially applied in Geotechnical engineering by [11] in the early 1990s. Many researchers in the past have successfully applied the soft computing techniques to model the geotechnical engineering problems such as slope stability and landslides [12], shear strength parameters and stress history [13], soil swelling and soil pressure [14], site characterization [15], lateral earth pressure [16], soil permeability [17], settlement [18-21], ultimate bearing capacity of regular plan shaped footing [22-29], ultimate bearing capacity of regular plan shaped footing (circular and square) with skirt [30-31] and ultimate bearing capacity of multi-edges footings without skirt using artificial neural network [9]. Similarly, the application of these techniques was explored in the other field of civil engineering by [32-41]. The literature presented above indicates that the soft computing technique such as ANN has been extensively used to model the bearing capacity of the regular plan shaped footings (with and without a skirt) and multi-edge footing (without a skirt). But no study is available for the unconventional H shaped skirted footing till date. The same is attempted in the present study. In this regard, the data for the regular shaped such as square, circular, rectangular and strip (up to $L/B = 2.5$) skirted footing was collected from the published literature. Using this data the ANN model to predict the bearing capacity ratio (BCR) was first developed. The various input variables used were non-dimensional skirt depth (D_s/B), friction angle of the sand (ϕ), ratio of interface friction angle to the friction angle of the sand (δ/ϕ) and length to width (L/B) ratio were considered as input variables with bearing capacity ratio as an output. This model for the BCR for the regular plan shaped skirted footings was later modified to predict the bearing capacity ratio of the H plan shaped multi-edge skirted footing with the introduction of the multiplication factor.

3. Soft computing techniques

3.1. Artificial Neural Network

ANN, initially introduced by [42], is the branch of artificial intelligence. ANN tries to imitate the nervous system and the function of the human brain. ANN modeling can differentiate complex nonlinear connections amongst the input and the output variables without any preceding expectations. Further, the ANN can use the raw data (input) without any need for manipulation or pre-processing which

makes the ANN more useful and less costly in comparison to the conservative techniques. An ANN is required to be trained before making any interpretation of the new information for which many algorithms were available in the literature. Among them, a feed-forward backpropagation algorithm is the utmost versatile [21,24,25,31,32,34] and efficient for the multilayer neural network. The back-propagation (BP) algorithm contains interconnected layers (input, hidden, and output). The output of the neuron or the node of the input layer was sent to a node in the hidden layer as an input, and the output of the neuron or the node of the hidden layer was sent finally to the output layer. The number of neurons in the hidden layers and the number of hidden layers are dependent on the problem in hand. Hence, researchers have resorted to a cumbersome trial and error procedure. All nodes (excluding the input layer) in the BP network were having an activation function and a bias node. The bias contains constant input. The activation function filters the summed output. Activation functions in ANN were used based on the objective. Computed vectors of the output corresponding to the solution of the problem, were created by the output layer. Typically, the input/output data were represented as vectors (named as training pairs). For the training pairs in the data, the process continues until the network error gets congregated to a brink which is defined using an error function (RMSE, root mean square error). The j^{th} neuron is linked to several inputs in the hidden layer as:

$$x_i = (x_1 + x_2 + x_3 + \dots + x_n) \quad (1)$$

Within the hidden layer, the net input (equation 2) will be:

$$N_j = \sum_{i=1}^n x_i y_{ij} + z_j \quad (2)$$

where:

x_i denotes the input units,

y_{ij} signifies the weights on the connection of the i^{th} input and j^{th} neuron,

z_j represents the bias node (optional) and

n stands for the number of input variables.

Logarithmic sigmoid function (equation 3) was used to calculate the output from the hidden layer:

$$f(S_j) = \frac{1}{1 + \exp(-mS_j)} \quad (3)$$

where:

S_j = input variables,

m = steepness constant,

the whole input to the k^{th} variable will be as per equation 4.

$$N_k = \sum_{i=1}^n y_{jk} S_j + z_k \quad (4)$$

where:

z_k signifies the bias node,

y_{jk} denotes the weight between the j^{th} neuron and the k^{th} output.

The entire output from the k^{th} variable will be as per equation 5.

$$S_k = f(N_k) \tag{5}$$

ANN uses weights and brinks to calculate its output. After this, a comparison is attempted between the desired output and the actual output. The error in the layer k corresponding to any output will then be calculated as per equation 6.

$$v_1 = t_k - S_k \tag{6}$$

where:

t_k signifies the predicted output,

S_k means the targeted output.

The total error has been calculated using equation 7.

$$F = 0.5 \sum_{k=1}^n (t_k - S_k)^2 \tag{7}$$

The training aimed to achieve optimal weights for the neural network as per equation 8 to reduce the error.

$$\nabla y_{jk} = -\psi \left(\frac{\delta F}{\delta y_{jk}} \right) \tag{8}$$

where,

F and ψ represent the error function and the learning rate respectively.

For the $(n+1)^{\text{th}}$ iteration, the updated weights were calculated as per equation 9.

$$w_{jk}(n+1) = w_{jk}(n) + \psi \nabla y_{jk}(n) \tag{9}$$

An identical procedure was adopted for connecting the hidden and the output layer. Further, during the training (input to the hidden and hidden to the output layer) of the network, the above procedure was repeated. A single step in the whole training pattern is known as an iteration. Hence, the number iterations are repeated to reach (an error is within a specified limit) the required output.

3.2. M5P model tree

M5P model tree proposed by [43] is based on a binary decision tree. This binary decision tree at the leaf node is having a series of linear regression functions. The divide and conquer technique was used to create a tree-based model. Model tree generation was carried out in two different stages. A decision tree was created in the first stage by splitting the data into subsets. These subsets were created based on the standard deviation of the class value, which reaches the node as a measure of the error. Then the expected

reduction in the error is calculated. The formula reported by [43,44] for the standard deviation reduction (SDR) was used to define the reduction in the error as per equation 10.

$$SDR = sd(T) - \sum \frac{|T_i|}{T} sd(T_i) \tag{10}$$

where:

T signifies a set of examples which reach the node,

T_i means a subset of examples which have the i^{th} outcome of the potential set,

sd signifies the standard deviation.

To make the node purest, the splitting process forces the child node to have a smaller value of the standard deviation in comparison to the parent node. After examination of all the possible splits and to maximize the expected error reduction, the M5P model tree chooses the split.

4. Data collection

A total of 162 numbers of data for the regular plan shaped footings on the sand was collected from the published literature [1-9] for the calculation of bearing capacity ratio. Collected data both for training and testing are given in Table 1 and Table 2 respectively. Further, the bearing capacity of the regular plan shaped footings with skirt depends on the skirt depth to width of the footing (D_s/B) ratio, angle of friction (ϕ) of the sand, the ratio of the interface friction angle to the friction angle of the sand (δ/ϕ), and length-to-width (L/B) ratio. Therefore, a model was developed considering all the four variables as input, whereas the output was the bearing capacity ratio (BCR) which is defined as:

$$BCR = \frac{[q_{sk}]_{(\phi, D_s/B, L/B, \delta/\phi)}}{[q_{su}]_{(\phi, L/B, \delta/\phi)}} \tag{11}$$

where:

$[q_{sk}]_{(\phi, D_s/B, L/B, \delta/\phi)}$ = Bearing capacity of skirted footing,

$[q_{su}]_{(\phi, L/B, \delta/\phi)}$ = Bearing capacity of unskirted footing.

Table 1.

Range of the data for regular-shaped skirted footings for training

Input parameters	Total data set			
	Min.	Max.	Avg.	Standard deviation
ϕ	33.02	46.00	39.29	3.57
D_s/B	0.00	2.00	0.57	0.52
L/B	1.00	2.50	1.37	0.51
δ/ϕ	0.59	1.00	0.76	0.16
BCR	1.00	6.25	1.98	1.03

Table 2. Range of the data for regular-shaped skirted footings for testing

Input parameters	Total data set			
	Min.	Max.	Avg.	Standard deviation
ϕ	33.36	46.00	38.01	6.37
D_s/B	0.00	2.00	0.65	0.51
L/B	0.51	2.50	1.42	0.55
δ/ϕ	0.15	1.00	0.76	0.17
BCR	0.88	4.64	2.06	0.97

The developed model was evaluated using six statistical parameters: correlation coefficient (r), coefficient of determination (R^2), mean square error (MSE), root mean square error (RMSE), mean absolute error (MAE), and mean absolute percentage error (MAPE).

5. Development of ANN model

Connection weights were generated on completion of the training of the network. Further, the mean square error (MSE) and the coefficient of determination (R^2) were significantly influenced by the number of neurons in the hidden layer. A variation of the number of neurons in the hidden layer and the MSE is shown in Figure 2. This figure reveals that up to the 8 numbers of neurons in the hidden layer, the MSE decreased and R^2 increased beyond which the trend was reversed. Keeping this in view, the neural network structure was finalized using 4 input layers – 1 hidden layer (with 8 hidden layer neuron) – 1 (output layer). ANN architecture through the diagram is shown in Figure 3. The mean square error is defined

$$MSE = \frac{\sum_{i=1}^n (BCR_i - BCR_F)^2}{n} \tag{12}$$

$$R^2 = \frac{D_1 - D_2}{D_1} \tag{13}$$

where:

$$D_1 = \sum_{i=1}^n (BCR_i - \overline{BCR})^2 \tag{14}$$

$$D_2 = \sum_{i=1}^n (BCR_i - BCR_i)^2 \tag{15}$$

where BCR_i , \overline{BCR} and BCR_F are the experimental, average of the experimental and predicted BCR, respectively; and n is the number of training data. An open-source WEKA software was used for modeling.

The next step in the ANN is to fix the number of optimum iterations. For this, the MSE was calculated for each lift (containing 10 iterations) and continued up to 250 numbers of iterations and the same was presented in Figure 4.

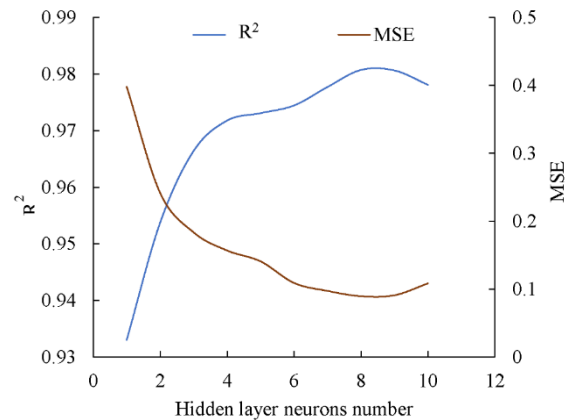


Fig. 2. Estimation of the optimum number of hidden layer neurons

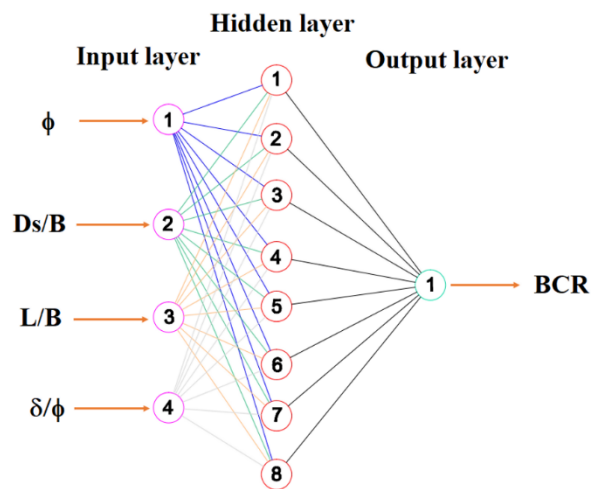


Fig. 3. Architecture of the ANN model

The study of Figure 4 reveals that at about 160 numbers of iterations, there is not much change in the MSE and the plot becomes parallel to a horizontal axis. Hence, 160 numbers of iterations were considered optimum for modeling. The BCR obtained from the neural network was compared with the actual BCR to verify the prediction accuracy of the ANN model. The comparison between the BCR estimated from the ANN, and the actual BCR for the training and the testing data were presented in Figures 5 and 6 respectively. Study of Figures 5 and 6 reveal that the calculated values of the coefficient of determination (R^2) were found to be 0.904 and 0.873, respectively, for the training and the testing data. Further, the accuracy of the developed model was assessed with other statistical parameters (correlation coefficient (r), MSE, RMSE, MAE and MAPE) for the training and the testing data which were tabulated in Table 3.

Table 3. Statistical parameters for ANN model

Statistical parameters	Training	Testing
r	0.99	0.99
R ²	0.90	0.87
MSE	0.09	0.10
RMSE	0.30	0.31
MAE	0.20	0.20
MAPE, %	10.41	11.03

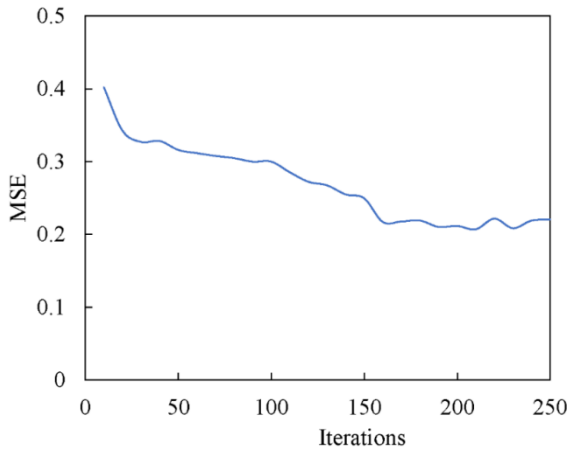


Fig. 4. Estimation of optimum iterations

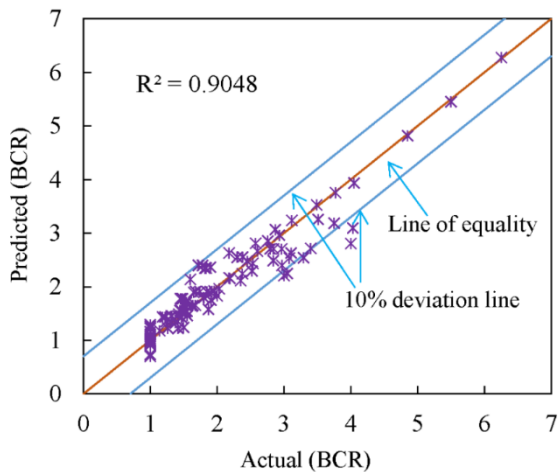


Fig. 5. Comparison between actual BCR with the one predicted from ANN for the training data

Table 3 reveals that all the statistical parameters were within the permissible range (readers may refer to [31] for the range of statistical parameters). After simulating the model for the optimal conditions, a matrix of the connection

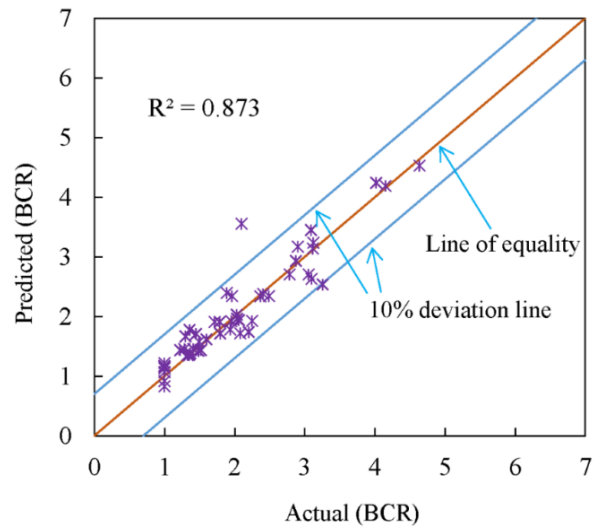


Fig. 6. Comparison between actual BCR with the one predicted from ANN for the testing data

weights between the input layers to hidden layer [x_{ji}], hidden layer to the output layer [y_{jk}], input bias [z_j] and the output bias [z_0] were presented in equations 16 to 20 below.

$$x_{ji} = \begin{bmatrix} x_{11} & x_{12} & x_{13} & x_{14} \\ x_{21} & x_{22} & x_{23} & x_{24} \\ x_{31} & x_{32} & x_{33} & x_{34} \\ x_{41} & x_{42} & x_{43} & x_{44} \\ x_{51} & x_{52} & x_{53} & x_{54} \\ x_{61} & x_{62} & x_{63} & x_{64} \\ x_{71} & x_{72} & x_{73} & x_{74} \\ x_{81} & x_{82} & x_{83} & x_{84} \end{bmatrix} \quad (16)$$

$$= \begin{bmatrix} 1.13 & -1.57 & -1.44 & -0.94 \\ 0.25 & 3.78 & 1.23 & -0.73 \\ -0.66 & -1.10 & 0.18 & 4.75 \\ -1.23 & -0.54 & 0.57 & -6.55 \\ -0.80 & -0.80 & -1.27 & 0.30 \\ 0.07 & 0.20 & 0.70 & 0.32 \\ 0.06 & 0.43 & 0.68 & 0.38 \\ -2.51 & 3.29 & -1.15 & 0.19 \end{bmatrix} \quad (17)$$

$$y_{jk} = \begin{bmatrix} y_{11} \\ y_{21} \\ y_{31} \\ y_{41} \\ y_{51} \\ y_{61} \\ y_{71} \\ y_{81} \end{bmatrix} = \begin{bmatrix} 0.09 \\ 0.31 \\ -1.00 \\ -2.29 \\ 0.27 \\ -2.04 \\ -5.89 \\ -3.11 \end{bmatrix} \quad (18)$$

$$z_j = \begin{bmatrix} z_1 \\ z_2 \\ z_3 \\ z_4 \\ z_5 \\ z_6 \\ z_7 \\ z_8 \end{bmatrix} = \begin{bmatrix} -0.26 \\ -0.25 \\ 2.17 \\ -1.08 \\ -1.11 \\ 1.60 \\ -1.50 \\ 0.34 \end{bmatrix} \quad (19)$$

$$z_0 = [-0.30] \quad (20)$$

where:

$[x_{ji}]$ = weight between j^{th} neuron of the hidden layer and i^{th} neuron in the input layer;

$[y_{jk}]$ = weight between the k^{th} layer of output neuron and j^{th} neuron in the hidden layer;

$[z_j]$ = j^{th} neuron of the hidden layer bias;

$[z_0]$ = output layer bias.

Therefore, it can be concluded that the neural network was trained properly and can be used to predict with reasonable accuracy.

5.1. Sensitivity analysis

This part of the study discusses the contribution of the individual variables on the bearing capacity ratio (output) by performing the sensitivity analysis. For this purpose, the methods (based on weight configuration) reported by [44,45] were used. In the first method [43], the connection weights of each of the hidden neurons in the hidden layer were divided into components. These components were associated with each input neuron. In the second method [45], the sum of the product of the final weights of the connections (input neuron to hidden neurons and hidden neurons to output BCR) for all the input neurons is calculated. The contribution of the individual variable corresponding to a given input is computed using Equation

21 and 22 for the first [44] and the second [45] methods respectively.

$$Q_{ik} = \frac{\sum_{j=1}^L \left(\frac{x_{ij}}{\sum_{r=1}^N x_{rj}} y_{jk} \right)}{\sum_{i=1}^N \left(\sum_{j=1}^h \left(\frac{x_{ij}}{\sum_{r=1}^N x_{rj}} y_{jk} \right) \right)} \quad (21)$$

where:

x_{ij} = connection weight between the hidden neuron j and the input neuron i ;

y_{jk} = connection weight between the output neuron k and the hidden neuron j ;

h = sum of the connection weights between the hidden neuron j and the N input neurons;

Q_{ik} = percentage of influence on the output O_k due to input variable I_i concerning the remaining input variables in a way that the sum of Q_{ik} provides a value of 100% for all the input variables.

$$IR_j = \sum_{k=1}^h x_{jk} \times x_k \quad (22)$$

Where:

x_{jk} = connection weight between k^{th} neuron of the hidden layer and j^{th} input variable;

x_k = connection weight between the single output neuron and the k^{th} neuron of a hidden layer;

IR_j = relative importance of the j^{th} neuron in the input layer

h = number of neurons in the hidden layer.

The relative influence of the individual variable on bearing capacity ratio (output) using Equation 21 and 22 was shown in Figure 7.

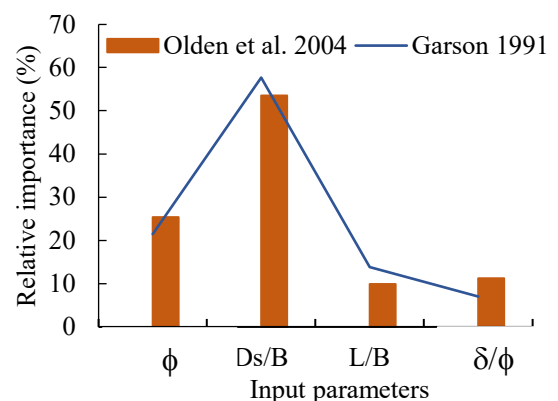


Fig. 7. Sensitivity analysis of the bearing capacity ratio following [44,45] method

Study of Figure 7 reveals that the D_s/B is significantly influencing the BCR (output). The other input variables (ϕ , δ/ϕ and L/B) were the next in this order affecting the BCR (output) using both the methods [44,45]. Thus, it is concluded that performing sensitivity analysis is an effective way to physically connect the input variables with the BCR (output).

5.2. Proposed model equation using ANN

After obtaining the final trained weights, a model equation was proposed in this section as per [46,47]. Taking into account the weights and biases given by equations (16)-(20), the ANN model takes the following form:

$$BCR = \left(\frac{[q_{sk}]_{(\phi, D_s/B, L/B, \delta/\phi)}}{[q_{su}]_{(\phi, L/B, \delta/\phi)}} \right) = f_n \left\{ z_0 + \sum_{i=1}^h \left[y_{jk} f_n \left(\sum_{i=1}^n x_{ji} E_i \right) \right] \right\} \quad (23)$$

where:

h = number of neurons in a hidden layer which is equal to 8 in this case

E_i = normalized inputs in the range of 0 to 1.

f_n = Activation function

n = number of input variables

The following steps [A_1 - A_8 and B_1 - B_8 uses Equations (24-31) and (32-39) respectively] were carried out for the development of the model equation using ANN. The final expression obtained was as per equation (40). This equation (40) provides a normalized BCR. Equations (41) and (42) provide the output BCR in de-normalized form.

$$A_1 = x_{11} \times \phi + x_{12} \times \frac{D_s}{B} + x_{13} \times \frac{L}{B} + x_{14} \times \frac{\delta}{\phi} + z_1 \quad (24)$$

$$A_2 = x_{21} \times \phi + x_{22} \times \frac{D_s}{B} + x_{23} \times \frac{L}{B} + x_{24} \times \frac{\delta}{\phi} + z_2 \quad (25)$$

$$A_3 = x_{31} \times \phi + x_{32} \times \frac{D_s}{B} + x_{33} \times \frac{L}{B} + x_{34} \times \frac{\delta}{\phi} + z_3 \quad (26)$$

$$A_4 = x_{41} \times \phi + x_{42} \times \frac{D_s}{B} + x_{43} \times \frac{L}{B} + x_{44} \times \frac{\delta}{\phi} + z_4 \quad (27)$$

$$A_5 = x_{51} \times \phi + x_{52} \times \frac{D_s}{B} + x_{53} \times \frac{L}{B} + x_{54} \times \frac{\delta}{\phi} + z_5 \quad (28)$$

$$A_6 = x_{61} \times \phi + x_{62} \times \frac{D_s}{B} + x_{63} \times \frac{L}{B} + x_{64} \times \frac{\delta}{\phi} + z_6 \quad (29)$$

$$A_7 = x_{71} \times \phi + x_{72} \times \frac{D_s}{B} + x_{73} \times \frac{L}{B} + x_{74} \times \frac{\delta}{\phi} + z_7 \quad (30)$$

$$A_8 = x_{81} \times \phi + x_{82} \times \frac{D_s}{B} + x_{83} \times \frac{L}{B} + x_{84} \times \frac{\delta}{\phi} + z_8 \quad (31)$$

$$B_1 = \frac{y_{11}}{1 + e^{-A_1}} \quad (32)$$

$$B_2 = \frac{y_{21}}{1 + e^{-A_2}} \quad (33)$$

$$B_3 = \frac{y_{31}}{1 + e^{-A_3}} \quad (34)$$

$$B_4 = \frac{y_{41}}{1 + e^{-A_4}} \quad (35)$$

$$B_5 = \frac{y_{51}}{1 + e^{-A_5}} \quad (36)$$

$$B_6 = \frac{y_{61}}{1 + e^{-A_6}} \quad (37)$$

$$B_7 = \frac{y_{71}}{1 + e^{-A_7}} \quad (38)$$

$$B_8 = \frac{y_{81}}{1 + e^{-A_8}} \quad (39)$$

$$R_1 = \left(\frac{[q_{sk}]_{(\phi, D_s/B, L/B, \delta/\phi)}}{[q_{su}]_{(\phi, L/B, \delta/\phi)}} \right) = BCR = B_1 + B_2 + B_3 + B_4 + B_5 + B_6 + B_7 + B_8 + z_0 \quad (40)$$

After de-normalization

$$\left(\frac{[q_{sk}]_{(\phi, D_s/B, L/B, \delta/\phi)}}{[q_{su}]_{(\phi, L/B, \delta/\phi)}} \right) = BCR = 0.5(BCR + 1) ([BCR]_{\max} - [BCR]_{\min}) + [BCR]_{\min} \quad (41)$$

$$\left(\frac{[q_{sk}]_{(\phi, D_s/B, L/B, \delta/\phi)}}{[q_{su}]_{(\phi, L/B, \delta/\phi)}} \right) = BCR = 0.5(BCR + 1)(5.25) + 1 \quad (42)$$

Based on the data collected from the literature, a model equation using ANN is proposed (Equation 42). This equation can be used to determine the ultimate bearing capacity of the regular plan shaped skirted footing on the sand. Figure 8 shows the comparison between the bearing capacity ratio (Equation 1) and the bearing capacity ratio obtained using ANN (Equation 42).

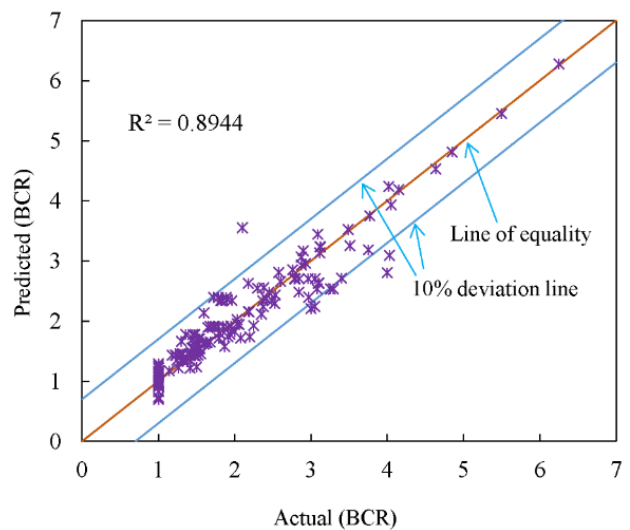


Fig. 8. Comparison between actual BCR and the one predicted using ANN

This figure reveals that the deviation between the predicted and the actual BCR using ANN was ± 10%. Therefore, the ANN can be effectively used for the prediction of the bearing capacity ratio of the regular plan shaped skirted footings.

6. Model development using M5P model tree

The equation for the BCR of the regular plan shaped skirted footing on sand using another soft computing technique (M5P model tree) was also developed, which is shown below as an equation 43.

$$\left(\frac{[q_{sk}]_{(\phi, Ds/B, L/B, \delta/\phi)}}{[q_{su}]_{(\phi, L/B, \delta/\phi)}} \right) = BCR = -1.75\phi + 1.66 \frac{Ds}{B} + 9.64 \frac{L}{B} - 7.35 \frac{\delta}{\phi} + 1.61 \tag{43}$$

The actual BCR versus predicted BCR plots were shown in Figure 9, and the statistical parameters (r, R², MSE, RMSE, MAE, and MAPE) were calculated and presented in Table 4. The study of Figure 9 and Table 4 reveals that the M5P model tree can predict the ultimate bearing capacity of the regular plan shaped skirted footing on the sand with moderate accuracy.

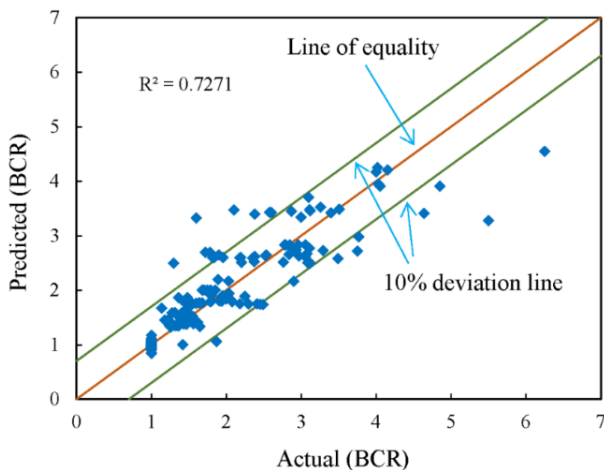


Fig. 9. Comparison between actual BCR and the one predicted using M5P model tree

Table 4. Statistical parameters for the M5P model tree

r	R ²	MSE	RMSE	MAE	MAPE, %
0.86	0.72	8.92	2.99	2.30	27.65

7. Comparison of developed models

To determine the bearing capacity of a regular plan shaped skirted footing in terms of BCR using ANN and M5P model, tree techniques were developed. The statistical parameters for the ANN model such as r, R², MSE, RMSE, MAE and MAPE for ANN model were 0.99, 0.90, 0.09, 0.30, 0.20 and 10.41; 0.99, 0.87, 0.10, 0.31, 0.20 and 11.03 for the training and the testing data respectively. Similarly, the statistical parameters such as r, R², MSE, RMSE, MAE, and MAPE for the M5P model were 0.86, 0.73, 8.92, 2.99, 2.30, and 27.65 respectively. These results reveal that the accuracy of the ANN model is superior to the one obtained using the M5P model tree technique.

8. Correlation between the BCR of regular and H plan shaped skirted footing on sand

To develop the multiplication factor (MF) for the H plan shaped skirted footing, [10] conducted laboratory plate load tests in a test tank (made with perspex sheet with dimensions 700 mm x 450 mm x 600 mm) to determine the bearing capacity of the H plan shaped skirted footing (made of mild steel with a thickness of 10 mm) on the sand by varying the relative density, δ/φ and the skirt depth using a test setup as shown schematically in Figure 10.

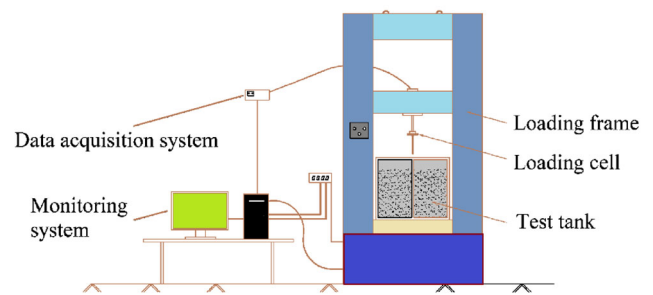


Fig. 10. Test setup

The H shaped skirted footing with different skirt depths is shown in Figure 11. For more details on the properties of the sand, sand placement procedure, insertion of footing, and other experimental details, readers may refer to [10]. The experimental data generated in this study was reported in [10] for the range of δ/φ = 0.60 to 0.99 and was tabulated in Table 5. This data was used to develop the multiplication factor (MF) to be multiplied with the BCR of the regular plan shaped skirted footing to arrive at the bearing capacity ratio

Table 5. Bearing capacity ratio for the H plan shaped footing with and without skirt (after [10])

D _s /B	Bearing capacity ratio at a relative density of							
	30 %		40 %		50 %		60 %	
	δ/φ = 0.60	δ/φ = 0.96	δ/φ = 0.61	δ/φ = 0.99	δ/φ = 0.61	δ/φ = 0.98	δ/φ = 0.65	δ/φ = 0.97
0	1.00	1.00	1.00	1.00	1.00	1.00	1.00	1.00
0.25	1.56	1.50	1.51	1.42	1.45	1.33	1.35	1.28
0.5	1.95	1.87	1.87	1.74	1.76	1.61	1.66	1.53
1	2.83	2.54	2.54	2.34	2.41	2.16	2.17	2.05
1.5	3.56	3.16	3.17	2.86	2.97	2.64	2.70	2.41



Fig. 11. H shaped skirted footing

of the H plan shaped skirted footing on the sand. The governing equations (Equations 44 and 45) for the ANN and M5P model tree are shown below.

$$\left(\frac{[q_{sk}]_{(\phi, D_s/B, L/B, \delta/\phi)}}{[q_{su}]_{(\phi, L/B, \delta/\phi)}} \right) = BCR_H = [0.5(BCR+1)(5.25)+1] \times MF_{ANN} \quad (44)$$

$$\left(\frac{[q_{sk}]_{(\phi, D_s/B, L/B, \delta/\phi)}}{[q_{su}]_{(\phi, L/B, \delta/\phi)}} \right) = BCR_H = \left[-1.75\phi + 1.66 \frac{D_s}{B} + 9.64 \frac{L}{B} - 7.35 \frac{\delta}{\phi} + 1.61 \right] \times MF_{M5P} \quad (45)$$

To obtain the multiplication factor for the H plan shaped skirted footing on the sand, the BCR_H of the H plan shaped footing was correlated to the bearing capacity ratio predicted from the ANN and M5P model tree and the multiplication factor obtained from this analysis was 1.06 and 1.09 respectively.

The BCR_H versus BCR_{H_ANN} plot is shown in Figure 12. Similarly, for the M5P model tree, the BCR_H versus BCR_{H_M5P} plot is shown in Figure 13. Study of the Figures 12 and 13 reveal that the R² for the BCR_H for the proposed ANN and M5P model for the H plan shaped skirted footing were 0.945 and 0.786, respectively. Hence, it can be concluded that the multiplication factor obtained using ANN is more accurate in comparison to the one obtained from the M5P model tree technique.

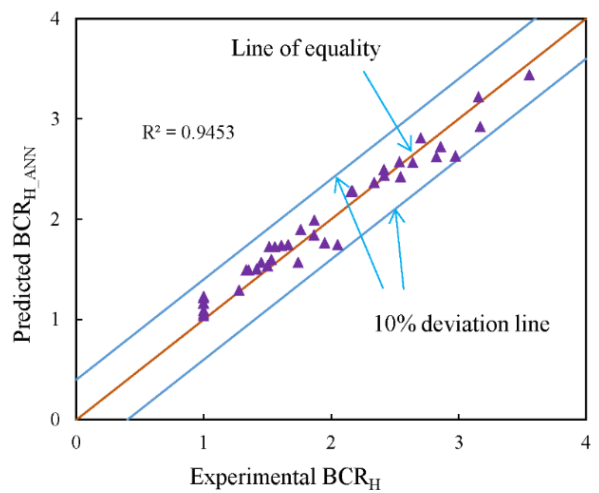


Fig. 12. Experimental BCR_H versus predicted BCR_{H_ANN} of the H plan shaped skirted footing

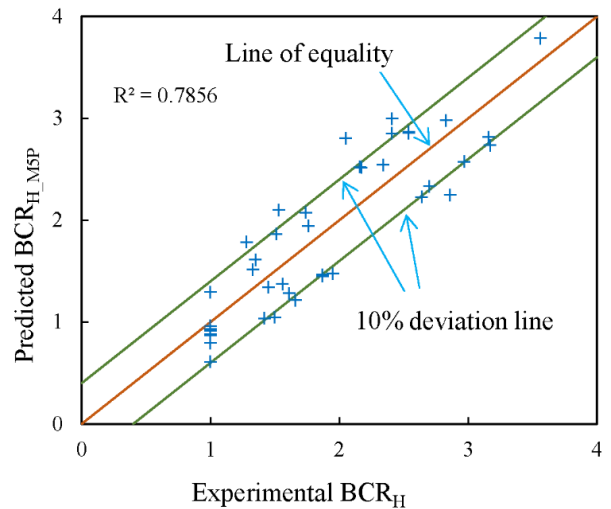


Fig. 13. Experimental BCR_H versus predicted BCR_{H_M5P} of H plan shaped skirted footing

9. Conclusions

The present work is aimed at developing the model equation for the non-dimensional bearing capacity ratio of the regular plan shaped skirted footing on sand using artificial neural networks and M5P model tree techniques. To obtain the model equations, the independent variables used were skirt depth to width of the footing ratio (D_s/B), friction angle (ϕ) of the sand, the ratio of the interface friction angle-to-the friction angle of the sand (δ/ϕ), and length-to-width (L/B) ratio of the regular plan shaped footing. The developed equation of the bearing capacity ratio for the regular plan shaped skirted footing was correlated to the bearing capacity ratio of the H plan shaped skirted footing using artificial neural network and M5P model tree technique and the following conclusions are put forward.

1. The comparison of the plots (actual versus predicted) concludes that the errors are distributed along the line of equality in the artificial neural network model. In contrast, the error distribution for the M5P model tree was little away from the line of equality. Hence, it is concluded that the prediction using a neural network model is more accurate in comparison to the one developed using the M5P model tree technique. The same is also evident from the statistical parameters (r , R^2 , MSE, RMSE, MAE, and MAPE).
2. The sensitivity analysis was conducted using the weights (generated during the development of the ANN model), to study the influence of the input variables on the output bearing capacity ratio. It is concluded that the influence of skirt depth to width of the footing ratio (D_s/B) was highest, i.e. 53.53%, followed by friction angle (ϕ) of the sand (25.35%).
3. Model equations developed to determine the BCR of regular plan shaped skirted footing on sand using artificial neural networks and M5P model tree technique. These developed equations were further correlated BCR_H of the H plan shaped skirted footing with a multiplication factor of 1.06 and 1.09, respectively.

On the whole, the paper has attempted to provide insight into the application of the soft computing techniques to predict the bearing capacity ratio of the H plan shaped skirted footing on the sand. It will help in the calculation of the bearing capacity of such unconventional geometry which otherwise requires expensive experimentation.

References

- [1] M.Y. Al-Aghbari, Y.E.A. Mohamedzein, Model testing of strip footings with structural skirts, Proceedings of the Institution of Civil Engineers – Ground Improvement 8/4 (2004) 171-177. DOI: <https://doi.org/10.1680/grim.2004.8.4.171>
- [2] M.Y. Al-Aghbari, Y.E.A. Mohamedzein, Improving the performance of circular foundations using structural skirts, Proceedings of the Institution of Civil Engineers – Ground Improvement 6/3 (2006) 125-132. DOI: <https://doi.org/10.1680/grim.2006.10.3.125>
- [3] M.Y. Al-Aghbari, R.K. Dutta, Performance of square footing with structural skirt resting on sand, Geomechanics and Geoengineering 3/4 (2008) 271-277. DOI: <https://doi.org/10.1080/17486020802509393>
- [4] R.N. Behera, C.R. Patra, Ultimate bearing capacity prediction of eccentrically inclined loaded strip footings, Geotechnical and Geological Engineering 36 (2018) 3029-3080. DOI: <https://doi.org/10.1007/s10706-018-0521-z>
- [5] R.N. Behera, C.R. Patra, N. Sivakugan, B.M. Das, Prediction of ultimate bearing capacity of eccentrically inclined loaded strip footing by ANN, part I, International Journal of Geotechnical Engineering 7/1 (2013) 36-44. DOI: <https://doi.org/10.1179/1938636212Z.00000000012>
- [6] R.N. Behera, C.R. Patra, N. Sivakugan, B.M. Das, Prediction of ultimate bearing capacity of eccentrically inclined loaded strip footing by ANN, part II, International Journal of Geotechnical Engineering 7/2 (2013) 165-172. DOI: <https://doi.org/10.1179/1938636213Z.00000000019>
- [7] W.Y. Byeon, S.R. Lee, Y.S. Kim, Application of flat DMT and ANN to Korean soft clay deposits for reliable estimation of undrained shear strength, International Journal of Offshore and Polar Engineering 16/10 (2006) 73-80.
- [8] N. Caglar, H. Arman, The applicability of neural networks in the determination of soil profiles, Bulletin of Engineering Geology and the Environment 66/3 (2007) 295-301. DOI: <https://doi.org/10.1007/s10064-006-0075-9>
- [9] B. Dawarci, M. Ornek, Y. Turedi, Analysis of multi-edge footings rested on loose and dense sand, Periodica Polytechnica Civil Engineering 58/4 (2014) 355-370. DOI: <https://doi.org/10.3311/PPci.2101>
- [10] R.K. Dutta, K. Dutta, S. Jeevanandham, Prediction of deviator stress of sand reinforced with waste plastic strips using neural network, International Journal of Geosynthetics and Ground Engineering 1/2 (2015) 1-12. DOI: <https://doi.org/10.1007/s40891-015-0013-7>
- [11] H.T. Eid, O.A. Alansari, A.M. Odeh, M.N. Nasr, H.A. Sadek, Comparative study on the behavior of square

- foundations resting on confined sand, Canadian Geotechnical Journal 46/4 (2009) 438-453. DOI: <https://doi.org/10.1139/T08-134>
- [12] Y. Erzin, Artificial neural networks approach for swell pressure versus soil suction behavior, Canadian Geotechnical Journal 44/10 (2007) 1215-1223. DOI: <https://doi.org/10.1139/T07-052>
- [13] G.D. Garson, Interpreting neural-network connection weights, AI Expert 6/4 (1991) 46-51.
- [14] T. Gnananandarao, V.N. Khatri, R.K. Dutta, Performance of multi-edge skirted footings resting on sand, Indian Geotech Journal 48/3 (2018) 510-519. DOI: <https://doi.org/10.1007/s40098-017-0270-6>
- [15] T. Gnananandarao, R.K. Dutta, V.N. Khatri, Application of artificial neural network to predict the settlement of shallow foundations on cohesionless soils, in: I.V. Anirudhan, V.B. Maji (eds.), Geotechnical Applications, IGC 2016 Volume 4, Lecture Notes in Civil Engineering Series, vol. 13, Springer, Singapore, 2019, 51-58. DOI: https://doi.org/10.1007/978-981-13-0368-5_6
- [16] A.T.C. Goh, Seismic liquefaction potential assessed by neural network, Journal of Geotechnical and Geoenvironmental Engineering 120/9 (1994) 1467-1480. DOI: [https://doi.org/10.1061/\(ASCE\)0733-9410\(1994\)120:9\(1467\)](https://doi.org/10.1061/(ASCE)0733-9410(1994)120:9(1467))
- [17] A.T.C. Goh, F.H. Kulhawy, C.G. Chua, Bayesian neural network analysis of undrained side resistance of drilled shafts, Journal of Geotechnical and Geoenvironmental Engineering 131/1 (2005) 84-93. DOI: [https://doi.org/10.1061/\(ASCE\)1090-0241\(2005\)131:1\(84\)](https://doi.org/10.1061/(ASCE)1090-0241(2005)131:1(84))
- [18] V.N. Khatri, S.P. Debbarma, R.K. Dutta, B. Mohanty, Pressure-settlement behavior of square and rectangular skirted footings resting on sand, Geomechanics and Engineering 12/4 (2017) 689-705. DOI: <https://doi.org/10.12989/gae.2017.12.4.689>
- [19] M.R. Mahmood, M.Y. Fattah, A. Khalaf, Experimental study on bearing capacity of skirted foundations on dry gypseous soil, International Journal of Civil Engineering and Technology 9/10 (2018) 1910-1922.
- [20] E. Momeni, D.J. Armaghani, S.A. Fatemi, R. Nazir, Prediction of bearing capacity of thin-walled foundation: a simulation approach, Engineering with Computers 34/2 (2018) 319-327. DOI: <https://doi.org/10.1007/s00366-017-0542-x>
- [21] W.S. McCulloch, W. Pitts, A logical calculus of ideas imminent in nervous activity, Bulletin of Mathematical Biophysics 5 (1943) 115-133. DOI: <https://doi.org/10.1007/BF02478259>
- [22] J.D. Olden, M.K. Joy, R.G. Death, An accurate comparison of methods for quantifying variable importance in artificial neural networks using simulated data, Ecological Modelling 178/3-4 (2004) 389-397. DOI: <https://doi.org/10.1016/j.ecolmodel.2004.03.013>
- [23] M. Omar, K. Hamad, M.A.I. Suwaidi, A. Shanableh, Developing artificial neural network models to predict allowable bearing capacity and elastic settlement of shallow foundation in Sharjah, United Arab Emirates, Arabian Journal of Geosciences 11/16 (2018) 464. DOI: <https://doi.org/10.1007/s12517-018-3828-4>
- [24] H.I. Park, Development of neural network model to estimate the permeability coefficient of soils, Marine Georesources and Geotechnology 29/4 (2011) 267-278. DOI: <https://doi.org/10.1080/1064119X.2011.554963>
- [25] J.R. Quinlan, Learning with continuous classes, Proceedings of the 5th Australian Joint Conference on Artificial Intelligence, Hobart, Australia, 1992, 343-348.
- [26] R. Sahu, C.R. Patra, N. Sivakugan, B.M. Das, Use of ANN and neuro fuzzy model to predict bearing capacity factor of strip footing resting on reinforced sand and subjected to inclined loading, International Journal of Geosynthetics and Ground Engineering 3 (2017) 29. DOI: <https://doi.org/10.1007/s40891-017-0102-x>
- [27] R. Sahu, C.R. Patra, N. Sivakugan, B.M. Das, Bearing capacity prediction of inclined loaded strip footing on reinforced sand by ANN, in: S. Shukla, E. Guler (eds), Advances in Reinforced Soil Structures, GeoMEast 2017, Sustainable Civil Infrastructures, Springer, Cham, 2017, 97-109. DOI: https://doi.org/10.1007/978-3-319-63570-5_9
- [28] R. Sahu, C.R. Patra, K. Sobhan, B.M. Das, Ultimate bearing capacity prediction of eccentrically loaded rectangular foundation on reinforced sand by ANN, in: M. Meguid, E. Guler, J. Giroud (eds), Advances in Geosynthetics Engineering, GeoMEast 2018, Sustainable Civil Infrastructures, Springer, Cham, 2019, 45-58. DOI: https://doi.org/10.1007/978-3-030-01944-0_5
- [29] N.M. Saleh, A.E. Alsaied, A.M. Elleboudy, Performance of skirted strip footing subjected to eccentric inclined load, Electronic Journal of Geotechnical Engineering 13 (2008) 11-13.
- [30] P. Samui, B. Kumar, Artificial neural network prediction of stability numbers for two-layered slopes with associated flow rule, The Electronic Journal of Geotechnical Engineering (2006) 1-42.

- [31] S.K. Sasmal, R.N. Behera, Prediction of combined static and cyclic load induced settlement of shallow strip footing on granular soil using artificial neural network, *International Journal of Geotechnical Engineering* (2018) 1-11.
DOI: <https://doi.org/10.1080/19386362.2018.1557384>
- [32] P. Sihag, F. Esmailbeiki, B. Singh, I. Ebtehaj, H. Bonakdari, Modeling unsaturated hydraulic conductivity by hybrid soft computing techniques, *Soft Computing* 23 (2019) 12897-12910. DOI: <https://doi.org/10.1007/s00500-019-03847-1>
- [33] B. Singh, P. Sihag, A. Tomar, A. Sehgal, Estimation of compressive strength of high-strength concrete by random forest and M5P model tree approaches, *Journal of Materials and Engineering Structures* 6 (2019) 583-592.
- [34] P. Sihag, M. Kumar, B. Singh, Assessment of infiltration models developed using soft computing techniques, *Geology, Ecology, and Landscapes* (2020) 1-11. DOI: <https://doi.org/10.1080/24749508.2020.1720475>
- [35] A. Sepahvand, B. Singh, P. Sihag, A.N. Samani, H. Ahmadi, S.F. Nia, Assessment of the various soft computing techniques to predict sodium absorption ratio (SAR), *ISH Journal of Hydraulic Engineering* (2019) 1-12.
DOI: <https://doi.org/10.1080/09715010.2019.1595185>
- [36] B. Singh, P. Sihag, K. Singh, Comparison of infiltration models in NIT Kurukshetra campus, *Applied Water Science* 8 (2018) 63.
DOI: <https://doi.org/10.1007/s13201-018-0708-8>
- [37] B. Singh, K. Singh, R. Kumar, P. Sihag, Future prediction and trend analysis of temperature of Haryana, *Journal of Indian Water Resources Society* 38/2 (2018) 24-27.
- [38] K. Singh, Dharmendra, Power density analysis by using soft computing techniques for microbial fuel cell, *Journal of Environmental Treatment Techniques* (2019) 1068-1073.
- [39] B. Singh, P. Sihag, K. Singh, Modelling of impact of water quality on infiltration rate of soil by random forest regression, *Modeling Earth Systems and Environment* 3 (2017) 999-1004.
DOI: <https://doi.org/10.1007/s40808-017-0347-3>
- [40] M. Kumar, N.K. Tiwari, S. Ranjan, Soft computing based predictive modelling of oxygen transfer performance of plunging hollow jets, *ISH Journal of Hydraulic Engineering* (2020) 1-11. DOI: <https://doi.org/10.1080/09715010.2020.1752831>
- [41] M. Kumar, N.K. Tiwari, S. Ranjan, Kernel function based regression approaches for estimating the oxygen transfer performance of plunging hollow jet aerator, *Journal of Achievements in Materials and Manufacturing Engineering* 95/2 (2019) 74-84. DOI: <https://doi.org/10.5604/01.3001.0013.7917>
- [42] M.A. Shahin, M.B. Jaksa, H.R. Maier, Artificial neural network-based settlement prediction formula for shallow foundations on granular soils, *Australian Geomechanics: Journal and News of the Australian Geomechanics Society* 37/4 (2002) 45-52.
- [43] M.A. Shahin, M.B. Jaksa, H.R. Maier, Artificial neural network applications in geotechnical engineering, *Australian Geomechanics* 36/1 (2011) 49-62.
- [44] B. Singh, P. Sihag, K. Singh, S. Kumar, Estimation of trapping efficiency of a vortex tube silt ejector, *International Journal of River Basin Management* (2018). DOI: <https://doi.org/10.1080/15715124.2018.1476367>
- [45] A. Soleimanbeigi, N. Hataf, Predicting ultimate bearing capacity of shallow foundations on reinforced cohesionless soils using artificial neural networks, *Geosynthetics International* 12/6 (2005) 321-332. DOI: <https://doi.org/10.1680/gein.2005.12.6.321>
- [46] E. Uncuoglu, M. Laman, A. Saglam, H.B. Kara, Prediction of lateral effective stresses in sand using artificial neural network, *Soils and Foundations* 48/2 (2008) 141-153.
DOI: <https://doi.org/10.3208/sandf.48.141>
- [47] A.Z.E. Wakil, Bearing capacity of skirt circular footing on sand, *Alexandria Engineering Journal* 52/3 (2013) 359-364.
DOI: <https://doi.org/10.1016/j.aej.2013.01.007>



© 2020 by the authors. Licensee International OCSCO World Press, Gliwice, Poland. This paper is an open access paper distributed under the terms and conditions of the Creative Commons Attribution-NonCommercial-NoDerivatives 4.0 International (CC BY-NC-ND 4.0) license (<https://creativecommons.org/licenses/by-nc-nd/4.0/deed.en>).